Selection of a Carbohydrate-Binding Domain with a Helix−Loop−Helix Structure[†]

Teruhiko Matsubara,[‡] Mie Iida,[‡] Takeshi Tsumuraya,[§] Ikuo Fujii,[§] and Toshinori Sato*,[‡]

Department of Biosciences and Informatics, Faculty of Science and Technology, Keio University, 3-14-1 Hiyoshi, Kouhoku-ku, Yokohama 223-8522, Japan, and Department of Biological Science, Graduate School of Science, Osaka Prefecture University, 1-2 Gakuen-cho, Sakai, Osaka 599-8570, Japan

Received January 16, 2008; Revised Manuscript Received March 19, 2008

ABSTRACT: We obtained a novel carbohydrate-binding peptide having a helix−loop−helix scaffold from a random peptide library. The helix−loop−helix peptide library randomized at five amino acid residues was displayed on the major coat protein of a filamentous phage. Affinity selection with a ganglioside, Galβ1−3GalNAcβ1−4(Neu5Acα2−3)Galβ1−4Glcβ1−1′Cer (GM1), gave positive phage clones. Surface plasmon resonance spectroscopy showed that a corresponding 35-mer synthetic peptide had high affinity for GM1 with a dissociation constant of 0.24 μM. This peptide preferentially binds to GM1 rather than asialo GM1 and GM2, suggesting that a terminal galactose and sialic acid are required for the binding as for cholera toxin. Circular dichroism spectroscopic studies indicated that a helical structure is important for the affinity and specificity. Furthermore, alanine scanning at randomized positions showed that arginine and phenylalanine play an especially important role in the recognition of carbohydrates. Such a de novo helix−loop−helix peptide would be available for the design of carbohydrate-binding proteins.

Lectins, antibodies, and proteins which are specific to carbohydrates serve as powerful tools in the identification of the physiological roles of glycoconjugates (*1*). Despite this, because glycotopes are poor immunogens, it is difficult to obtain antiglycan and antiglycolipid antibodies (*2, 3*). Approximately two-thirds of carbohydrate-binding antibodies are IgM (*2*), their affinity and specificity not always being sufficient in clinical use as a glycan probe. To overcome this, the affinity of antibodies has been improved through selection from phage-display libraries over the past decade (*4*). The affinity of monoclonal antibodies against oligosaccharides of Lewis^X (*5*), sialyl Lewis^X (*6*), α-galactosyl epitope (*7*), Thomsen-Friedenreich antigen (*8*), Galβ1−3GalNAcβ1−4Galβ1−4Glcβ1−1′Cer (asialo GM1)[1] (*3*), and Neu5Gcα2−3Galβ1−4Glcβ1−1′Cer (*N*-glycoyl GM3) (*9*) has improved. When it comes to lectin (*10, 11*) and hemagglutinin (*12, 13*), attempts to change binding specificity through mutation have been reported.

An alternative strategy might have great potential in the engineering of tailor-made artificial carbohydrate-binding proteins. Research groups have adopted various structural motifs for the de novo design of polypeptides such as metalloproteins (*14*), catalysts (*15, 16*), and bacteriorhodopsin (*17*). Random library-based selection and evolution with structural scaffolds using display technologies have provided proteins that target specific molecules (*18, 19*). In this study, a stable helix−loop−helix structure was chosen to construct an artificial carbohydrate-binding domain. Helix-based motifs are frequently conserved in proteins during molecular evolution (*20*). Selection from a randomized peptide library with the helix-type scaffold would give peptides that play a role as a carbohydrate-binding domain.

The ganglioside GM1 is well-known as a receptor of cholera toxin B subunit (CTB) (*21, 22*) and is often used as a marker of lipid rafts (*23*). Yanagisawa noted that GM1 is correlated with the accumulation of β-amyloid in cases of Alzheimer's disease (*24*). The development of GM1-binding molecules is required for investigation of the localization and roles of GM1 on the cell surface. Our previous selection from a random library showed a pentadecapeptide, p3, with affinity for a GM1 pentasaccharide with a dissociation constant (K_d) of 1.2 μM (*25, 26*). This peptide was specific to GM1 as well as CTB, but the binding affinity of the peptide was lower than that of CTB ($K_d = 10^{-8}-10^{-12}$ M) (*22*). Two-dimensional nuclear magnetic resonance (NMR) experiments showed that a conformational change of this peptide occurred during the binding to GM1 (*27*). To decrease the entropic loss caused by the conformational change, a helix-type scaffold was adopted for the selection. Five amino acids at the C-terminal helix of the helix−loop−helix scaffold were randomized to identify the GM1-specific peptide sequences. Phage display selection, alanine scanning, and circular dichroism experiments indicated the peptide to be specific

[†] This work was supported by a Grant-in-aid for the Encouragement of Young Scientists (17750166, T.M.) from the Ministry of Education, Culture, Sports, Science and Technology of the Japanese Government.

* To whom correspondence should be addressed: Department of Biosciences and Informatics, Faculty of Science and Technology, Keio University, 3-14-1 Hiyoshi, Kouhoku-ku, Yokohama 223-8522, Japan. Phone: +81-45-566-1771. Fax: +81-45-566-1447. E-mail: sato@bio.keio.ac.jp.

[‡] Keio University.

[§] Osaka Prefecture University.

[1] Abbreviations: GSL, glycosphingolipid; GM1, Galβ1−3GalNAcβ1−4(Neu5Acα2−3)Galβ1−4Glcβ1−1′Cer; GM2, GalNAcβ1−4(Neu5Acα2−3)Galβ1−4Glcβ1−1′Cer; asialo GM1, Galβ1−3GalNAcβ1−4Galβ1−4Glcβ1−1′Cer; GlcCer, Glcβ1−1′Cer; CTB, cholera toxin B subunit; K_d, dissociation constant; NMR, nuclear magnetic resonance; CFU, colony-forming units; PBS, phosphate-buffered saline; TBS, Tris-buffered saline; BSA, bovine serum albumin; ELISA, enzyme-linked immunosorbent assay; CD, circular dichroism; SPR, surface plasmon resonance; RU, resonance units; R_{max}, maximum resonance; R_{eq}, equilibrium resonance units; ΔG, Gibbs free energy change.

10.1021/bi8000837 CCC: $40.75
Published on Web 06/10/2008

to GM1 and the helical conformation to be necessary for the specific binding.

EXPERIMENTAL PROCEDURES

Materials. Gangliosides and glycosphingolipids (GSLs), Galβ1−3GalNAcβ1−4(Neu5Acα2−3)Galβ1−4Glcβ1−1′Cer (GM1), GalNAcβ1−4(Neu5Acα2−3)Galβ1−4Glcβ1−1′Cer (GM2), Galβ1−3GalNAcβ1−4Galβ1−4Glcβ1−1′Cer (asialo GM1), and Glcβ1−1′Cer (GlcCer) were obtained from Sigma-Aldrich Co. (St. Louis, MO). Anti-fd bacteriophage antibody, peroxidase-conjugated anti-rabbit IgG antibody, and peroxidase-conjugated cholera toxin B subunit (CTB) were obtained from Sigma-Aldrich. XL1-blue cell and helper phage (VCSM13) were obtained from Stratagene Co. (La Jolla, CA).

Phage Display Library. A random library of a helix−loop−helix peptide, AELAALEAELAALE-G_7-KLXXLKXKLXX-LKA, was constructed using a pComb8 system (*28*). This library was displayed on major coat protein VIII of a filamentous phage with a GGSSA spacer and GAPVPYP-DPLEPR (E-tag). We estimated the library has 3.2×10^7 recombinants, which is enough diversity to cover five randomized amino acids ($20^5 = 3.2 \times 10^6$).

Affinity Selection with GM1. For affinity selection, a ganglioside GM1 monolayer was prepared at the air−water interface in a Langmuir trough and immobilized onto a plastic plate (code 174950, Nunc) as reported previously with a minor modification (*25, 26*). The phage library (5×10^9 CFU) was incubated with GM1 in 200 μL of phosphate-buffered saline (PBS) at pH 6.0 ([phage] = 0.041 nM). After 30 min, the GM1 plate was washed three times to remove unbound phages. Bound phages were eluted for 15 min with glycine-HCl buffer (pH 2), and the eluate was neutralized with Tris-HCl buffer at pH 9.1. To estimate the phage number collected, a small portion of the eluate was saved and used for titering. *Escherichia coli* XL1-blue cells were infected with the phages in SB medium incubated for 30 min at 37 °C. After the addition of ampicillin, the transformed cells were grown for 1 h at 37 °C. The phages were rescued by adding a VCSM13 helper phage and further amplified overnight. The phages amplified were collected and purified with polyethylene glycol and NaCl for the next round. This process was repeated seven or nine times. After the last round of affinity selection, the titering plate was used to isolate individual phage clones. Each phagemid cloned was purified with a QIAprep Spin Miniprep Kit (QIAGEN Inc.) and used as a template for sequencing to deduce the amino acid sequence.

Peptide Synthesis and Purification. Peptides (peptide amides) were synthesized with a solid-phase peptide synthesizer (model 433A, Applied Biosystems) using 9-fluorenylmethoxycarbonyl (Fmoc) chemistry. The peptides were purified by reversed-phase high-performance liquid chromatography (C_{18} column, 250 mm × 20 mm inside diameter) with a linear gradient of water containing 0.1% trifluoroacetic acid (TFA) and acetonitrile containing 0.1% TFA at a flow rate of 10 mL/min. The major fractions were lyophilized, and the peptides were characterized by matrix-assisted laser desorption ionization time-of-flight mass spectrometry (autoflex, Bruker Daltonics, Inc.) using a matrix of α-cyano-4-hydroxycinnamic acid.

Circular Dichroism (CD) Spectroscopy. CD spectroscopy was performed on a Jasco J-820 spectropolarimeter using a 1 mm cuvette. Spectra were collected from 260 to 190 nm every 0.2 nm. The peptide concentrations were determined by measuring tyrosine absorbance (the molar absorbance coefficient at 257 nm equals 1450 M^{-1} cm^{-1}). A peptide solution (100 μM) was prepared with Tris-buffered saline (TBS) (50 mM Tris-HCl and 150 mM NaCl) at pH 7.5. The CD spectra are reported as mean residue ellipticity ([θ]) in degrees per square centimeter per decimole. The α-helical content was calculated from the following equation (*29*).

$$\alpha\text{-helical content} = (-[\theta]_{222} + 2340)/30300$$

Surface Plasmon Resonance (SPR) Analysis. The affinity of peptides for glycolipids was determined by SPR using a Biacore X biosensor system (Biacore International). The glycolipid monolayer was immobilized on a bare gold sensor chip (code BR-1004-05, Biacore International), and this chip was docked into the instrument. All measurements were carried out in TBS (pH 7.5) which was filtered (0.22 μm) and degassed prior to use. After the docking, TBS was injected over the chip at a flow rate of 10 μL/min for 30−40 min. Analyses were performed at 25 °C and with a flow rate of 5 μL/min for the determination of equilibrium binding. The sensor chip surfaces were regenerated with 4 M $MgCl_2$ for 8 min.

Binding affinity was calculated from a Scatchard analysis of equilibrium binding using the equation

$$R_{eq}/[\text{peptide}] = R_{max}/K_d - R_{eq}/K_d$$

where [peptide], R_{max}, and K_d are the concentration of peptide, the maximum resonance, and the dissociation constant, respectively. The resonances in the association phase at 500−600 s were used as the equilibrium resonance units (R_{eq}). The average R_{eq} values were plotted in the form R_{eq}/[peptide] versus R_{eq}, and K_d and R_{max} were calculated from the slope and intercept of the linear relationship, respectively. The peptide concentration range (1−20 μM) in which the peptide amounts were analyzed as a single interaction by a Scatchard plot was used to determine K_d values. In the case of B72, the concentrations of 1−10 μM were used for the analysis, since the multilayer adsorption was observed at 20 μM and reliable signals were not detected below 1 μM.

Molecular Modeling. Molecular modeling was performed using the InsightII/Discover3 system (Accelrys, Inc.). The peptide amide Ct5 was built using the Biopolymer module in InsightII, where the main chains of 1−14 and 22−36 residues are taken as the helical structure and the chain of 15−21 residues is extended. Simple minimization was performed using Discover3. To obtain peptide B72, substitutions of four alanines with Lys24, Arg28, Arg31, and Phe32 were made in Ct5 using the Biopolymer module. After the minimization, the final structure was used for the drawing shown in Figure 8. Crystallographic coordinates of the X-ray structure of pentasaccharide GM1 were obtained from the Protein Data Bank (entry 3CHB). The B72 peptide and GM1 pentasaccharide were superimposed.

RESULTS

Helix−Loop−Helix Design. The helix−loop−helix scaffold is composed of two helical sequences with seven

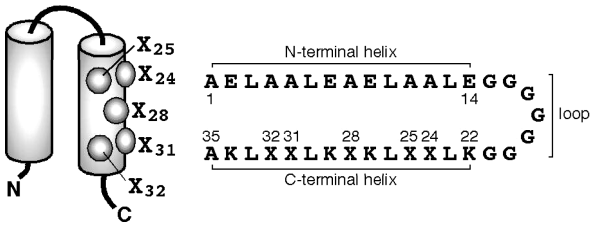

FIGURE 1: Structure of the helix−loop−helix library. An illustration of the helix−loop−helix library is shown at the left. Five randomized positions are arranged in the C-terminal helix, where X is a randomized position. The amino acid sequence of the helix−loop−helix peptide library is shown at the right.

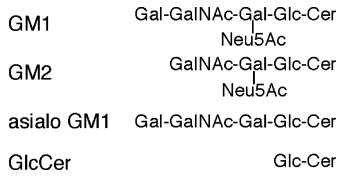

FIGURE 2: Schematic representation of gangliosides and GSLs employed in this study. Glc, glucose; Gal, galactose; GalNAc, *N*-acetylgalactosamine; Neu5Ac, *N*-acetylneuraminic acid; Cer, ceramide.

glycines as a spacer (Figure 1) (*30*). Leucines, glutamic acids, and lysines were positioned to stabilize the helical structure through hydrophobic interaction and the formation of salt bridges. We prepared a helix−loop−helix library for phage display selection with random substitutions at positions 24, 25, 28, 31, and 32 (*31*). The substituted residues were positioned outside of the C-terminal helix.

Phage Display Selection against GM1. The selection of peptides with affinity for ganglioside GM1 (Figure 2) was carried out as reported with minor revisions (*25*). Briefly, a GM1 monolayer was prepared at the air−water interface with a Langmuir trough and transferred to a plastic plate. The phage library was incubated with GM1 on the plate, and the bound phages were eluted under acid conditions. The phages obtained were amplified, purified, and subjected to another round. After seven and nine rounds of selection, 16 and 20 clones were isolated, respectively. The phage ELISA was used to identify the clones that have affinity for GM1 (Supporting Information, Figure S1). The first screening of 36 phage clones was performed via an ELISA, and then 13 clones were chosen for further investigation. To know the binding selectivity of 13 clones, K_d values for GM3 and GalCer were also investigated (data not shown). A914 and B72 were found to have high affinity for GM1 with K_d values of 0.075 and 0.13 nM, respectively, and exhibited a higher affinity than for GM3 and GalCer (Supporting Information, Table S1).

Binding Affinity and Helical Structure of Peptides. To analyze their affinity, these peptides were chemically synthesized (C-terminus amidated). To estimate the peptide concentration in buffer, tyrosine was added at the C-terminus of the peptide (Table 1). The binding of these peptides was characterized by the surface plasmon resonance method. Figure 3A shows typical sensorgrams of peptides A914, B72, and Ct5 at 10 μM in TBS (pH 7.5). Ct5 is a control peptide in which all sites randomized in the library are changed to alanines. The amount of B72 bound to GM1 was greater than that of other peptides and increased as the peptide concentration increased (Figure 3B). However, the kinetics of binding was not analyzed due to the rapid association and dissociation phases observed. Then, equilibrium binding experiments were performed to calculate K_d values using Scatchard plots; the K_d was 2.9 μM for A914, 0.24 μM for B72, and 11 μM for Ct5 (Table 1 and Figure 4). The binding affinity of B72 was 25-fold higher than that of the control Ct5. The R_{max} values for B72, Ct5, and B72-h, which is the C-terminal half of B72 containing five residues identified, were 280, 268, and 145 RU, respectively. These amounts bound to GM1 approximately corresponded to their molecular weights. However, A914 showed low affinity (2.9 μM) and small amounts (151 RU) against GM1, though the A914 phage clone had the same affinity for GM1 as the B72 clone (Table S1). Such a discrepancy between synthetic peptides and phage clones is often observed (*25, 32*). The binding preference of the selected peptides depends on the method of measurement. Then, on the basis of the results in Table 1, we chose B72 for further characterization. The K_d value of a 15-mer peptide, p3, selected previously was 1.2 μM (*26*). B72 exhibited greater (5-fold) affinity for GM1 than the nonhelical peptide p3. Lectins, toxins, and antibodies have several carbohydrate-binding domains (*33*). A multivalent B72 as tandem repeats or tentacle-type multimers would enhance the binding affinity (*34*).

To clarify how the helix of B72 is affected upon carbohydrate recognition, the secondary structure of B72 was investigated by CD spectroscopy. The CD spectra of B72 and Ct5 exhibited two minima at 208 and 222 nm, indicating a typical α-helical structure (Figure 5) (*35*). The mean residue ellipticity at 222 nm was −10471 deg cm^2 dmol^{-1} for B72 and −16040 deg cm^2 dmol^{-1} for Ct5. The helical content was estimated to be 42% for B72 and 61% for Ct5 (*29*). B72-h took no helical structure and had a lower affinity (K_d = 5.0 μM) than full-length B72 (K_d = 0.24 μM) (Table 1). These results suggest that the binding of B72 to GM1 was influenced by its secondary structure.

Binding Specificity of Peptides. The specificity with which B72, Ct5, and B72-h bind various glycolipids is shown in Figure 6 and summarized in Table 2. The affinity of B72 was 0.016- and 0.073-fold lower for GM2 and asialo GM1 than for GM1, respectively (15 μM for GM2 and 3.3 μM for asialo GM1). The binding preference (GM1 ≫ asialo GM1 > GM2) of B72 was in good agreement with that of p3 (*26*). The profile of the binding of Ct5 to GM1 was no different from that of the binding to other glycolipids, and the amount of B72-h bound to GM1 declined to the same level as that bound to GlcCer (as nonspecific binding) (Figure 6). These results suggested that the helical conformation and the five residues in B72 were crucial for the specificity for GM1.

Alanine Scanning. To determine the contribution of the five residues in B72, four alanine-substituted mutants of B72 were synthesized (B72-1, B72-2, B72-3, and B72-4) (Table 3). Single-alanine substitutions at positions 24, 28, 31, and 32 are predicted to alter the GM1 binding profile and helical conformation. The amount of peptide bound to GM1 was affected by all alanine substitutions (Table 3, Figure 7A, and Figure S2). Notably, the replacement of Arg31 (B72-3) and Phe32 (B72-4) with Ala markedly decreases the affinity for GM1; the amounts of B72-3 (67 RU at 5 μM) and B72-4 (54 RU) were 4−5-fold smaller than the amount of B72 (261 RU). The amounts of these mutants decreased to the same level as the control peptide, Ct5 (80 ± 23 RU at 5 μM) (Figure 6). It was suggested that Arg31 and Phe32 among

Table 1: Affinity of Synthetic Peptides for GM1

code	peptide structure [a]	molecular weight	R_{max} (RU)	K_d (μM)	relative affinity [b]
A914	AELAALEAELAALEGGGGGGGKLQELKTKLAALKAY-NH_2	3512.02	151	2.9	0.083
B72	AELAALEAELAALEGGGGGGGKLKALKRKLRFLKAY-NH_2	3670.31	280	0.24	1.0
B72-h	GGGKLKALKRKLRFLKAY-NH_2	1743.14	145	5.0	0.048
Ct5	AELAALEAELAALEGGGGGGGKLAALKAKLAALKAY-NH_2	3366.90	268	11	0.022

[a] Random positions are underlined. [b] Ratio to B72 peptide.

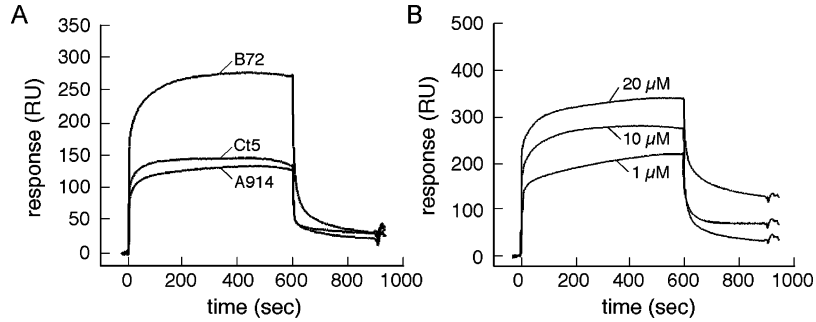

FIGURE 3: SPR sensorgrams for the interaction of peptides with GM1. (A) Overlay plot of the binding of A914, B72, and Ct5 at 10 μM. (B) Overlay plot of the binding of B72 at 1, 10, and 20 μM. Responses in RU are plotted vs time in seconds. Association (0−600 s) and dissociation (600−900 s) phases are shown.

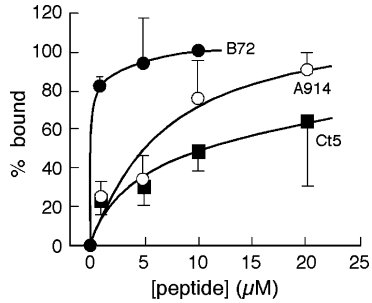

FIGURE 4: Amounts of A914, B72, and Ct5 bound to GM1 at various peptide concentrations observed by SPR spectroscopy. % bound, $(R_{eq}/R_{max}) \times 100$; R_{eq}, equilibrium response units at 500−600 s in the association phase; R_{max}, maximum response calculated from Scatchard plots (data not shown). The data are average values ± the standard deviation ($n = 2-4$).

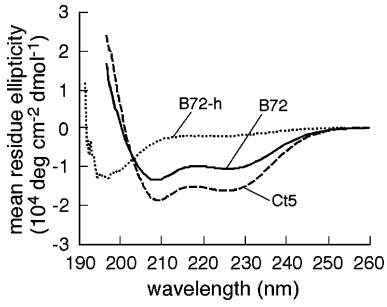

FIGURE 5: CD spectra of B72 (—), B72-h (•••), and Ct5 (---) in TBS at pH 7.5. The peptide concentration was 100 μM.

the four amino acid residues strongly contributed to the binding. In our previous studies, arginines and hydrophobic amino acids had been found in the motif shared among GM1-binding peptides (*25, 26*). These results were consistent with our previous papers.

To determine the influence of alanine substitutions on the helical conformation, CD spectra of these mutants were measured (Figure 7B). The two maxima at 208 and 222 nm were found in all the mutants, which indicates that the helical structure was maintained. The mean residue ellipticity at 222 nm of B72 mutants decreased except for that of B72-2; indeed, the α-helical content increased (65, 34, 59, and 48% for B72-1, B72-2, B72-3, and B72-4, respectively). Alanine is a stabilizer of helices, so an enhancement of helicity with alanine substitutions is reasonable (*36*). The CD spectra indicated that the decreases in affinity for GM1 are due to the loss of side chains of residues identified, and not due to disruption of the helical conformation.

DISCUSSION

The development of carbohydrate-binding molecules like lectins, toxins, and antibodies would greatly contribute to the evolution of glycoscience and glycotechnology. Especially for functional analyses of glycoconjugates, the need for carbohydrate-binding molecules will increase with progress in glycobiology (*37−41*). Recently developed selection technology, including the use of genomic and random libraries, has provided various repertories of carbohydrate-binding molecules (*42*). Lectin mutations, antibody libraries, and peptide libraries are beneficial sources. We have so far identified carbohydrate-binding molecules, regardless of natural sequences. We previously identified GM1-binding pentadecapeptides (15-mer peptides) from a random peptide library, one of which, p3, was specific to GM1 with a K_d of 1.2 μM (*25, 26*). This peptide exhibited unique recognition, including specific binding of the high-density GM1 domain. NMR analyses indicated that p3 underwent a conformational change on binding to GM1 (induced fit) (*27*). N-Terminal and C-terminal residues of p3 are flexible in the free state but are restricted once the carbohydrate−peptide interaction occurs. The energy of this binding could be used to overcome the entropy cost for this change. If the peptide conformation is rigid, no binding energy would have to be expended to pay the cost of this folding. We

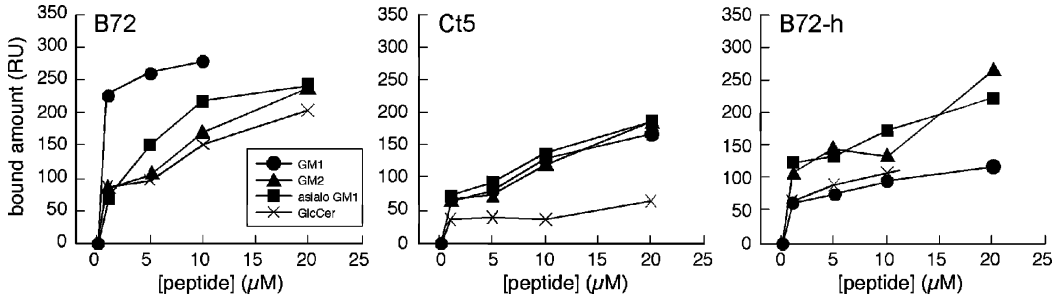

FIGURE 6: Amounts of B72, Ct5, and B72-h peptides bound to gangliosides and GSLs observed by SPR spectroscopy.

Table 2: Affinity of Synthetic Peptides for GM1, GM2, Asialo GM1, and GlcCer

peptide	glycolipid	R_{max} (RU)	K_d (μM)	relative affinity[a]
B72	GM1	280	0.24	1.0
	GM2	418	15	0.016
	asialo GM1	278	3.3	0.073
	GlcCer	322	12	0.020
Ct5	GM1	268	11	1.0
	GM2	377	21	0.52
	asialo GM1	275	9.9	1.1
	GlcCer	nd[b]	nd[b]	nd[b]
B72-h	GM1	145	5.0	1.0
	GM2	274	2.1	2.4
	asialo GM1	285	5.9	0.85
	GlcCer	110	0.77	6.5

[a] Ratio to GM1. [b] Not detectable.

therefore designed a novel carbohydrate-binding peptide with a structural scaffold in this study.

A helical conformation is the only structure that we can design. A helix−loop−helix (or helix−turn−helix) scaffold allows a peptide to form a stable helical structure. Fujii et al. designed a helix−loop−helix peptide library; the helix outside of five residues at 24, 25, 28, 31, and 32 was randomized to give a peptide library (*31*). The N-terminal residues interact with the C-terminus to stabilize the α-helical structure; therefore, this peptide is a monomer and does not form a dimer. They previously identified peptide agonists of the cytokine receptor and granulocyte colony-stimulating factor receptor using helix−loop−helix libraries (unpublished data). In this study, we conferred the ability to recognize carbohydrates on this peptide. The selection procedure followed that previously reported by us; a glycolipid monolayer was immobilized onto a plate and incubated with the phage library (*25*). This method allows the suppression of nonspecific interaction of phage particles with the lipid portion of the glycolipid and the plate surface exposed. The phage particles therefore interact with only the exposed carbohydrate portion of the glycolipid. The two GM1-positive clones, A914 and B72, were identified via a phage ELISA and were chemically synthesized. A synthetic B72 peptide showed specific binding to GM1 with a K_d of 0.24 μM and was found to have the highest affinity for GM1 as suggested by the phage ELISA (Table 1). The K_d value of Ct5, as a control peptide, was 11 μM, and Ct5 exhibited no specificity (Table 2 and Figure 6). This is because the helix−loop−helix scaffold contains several charged amino acids, glutamic acids (positions 2, 7, 9, and 14), and lysines (positions 22, 27, 29, and 34). These amino acids are able to interact nonspecifically with carbohydrates through hydrogen binding and/or salt bridges. These nonspecific interactions contributed to the binding affinity but were not involved directly in the specific interaction between the peptide and GM1 oligosaccharide. Therefore, the five amino acids, Lys24, Ala25, Arg28, Arg31, and Phe31, would be very important for the specific recognition of GM1. Furthermore, to determine whether formation of a helix is essential for binding, we designed a B72-h peptide that is the 18 C-terminal residues containing the five amino acids. The CD spectrum of B72-h exhibited an unordered structure (Figure 5). The five amino acid residues are therefore randomly arranged, and the orientation of these side chains would not be restricted. As expected, B72-h lost affinity and selectivity for GM1 (K_d = 5.0 μM) (Table 2 and Figure 6). These results indicate that the helical conformation of B72 is essential for the recognition of GM1.

Next, alanine-substituted mutants of B72 were used to identify the contributions of the selected amino acid residues to the binding to GM1. CD spectra indicated that replacing Lys24, Arg31, and Phe32 with alanine in the B72 peptide did not affect the helical conformation (Figure 7B). The substitution of Arg31 and Phe32 with alanine drastically changed the affinity (Figure 7A and Table 3), which indicates that these residues are essential for GM1's recognition. These residues would be arranged in the C-terminal helix (Figure 1). We previously identified the GM1-binding motif, (W/F)RxL(xP/Px)xFxx(Rx/xR)xP, and the binding of p3 mutants also showed that Arg and hydrophobic residues (Trp and Phe) contributed to the binding (*26*). Polar and aromatic amino acids often play important roles at carbohydrate-binding sites, because carbohydrate−protein interaction is achieved by a combination of hydrophobic interaction and hydrogen bonding (*33, 43*). The results of alanine scanning were well consistent with our previous results (*26*).

To estimate how much these five amino acids and the helical conformation contribute to formation of the B72−GM1 complex, the Gibbs free energy change (ΔG) upon formation of the complex was calculated from the K_d values. The ΔG values were calculated using the equation $\Delta G = -RT \ln K_d$, where T = 298 K. The difference in ΔG values between the Ct5−GM1 complex (−28.3 kJ/mol) and the B72−GM1 complex (−37.8 kJ/mol) was 9.5 kJ/mol (Figure 8). This energy difference is thought to be due to the five residues, because the only difference between the B72 and Ct5 sequences is these residues. Since the ΔG value of the B72-h−GM1 complex was −30.2 kJ/mol, the distribution of the helical conformation with the presence of the N-terminal half might be estimated to be 7.5 kJ/mol. These energy differences, 9.5 and 7.5 kJ/mol, suggest that both the five residues and the helical conformation were required for the suitable spatial arrangement of five residues on the helix to achieve the specific B72−GM1 interaction.

Table 3: Amounts of Synthetic Peptides Bound to GM1

code	peptide structure [a]	R_{eq} (RU) [b]	relative amount [c]
B72	AELAALEAELAALEGGGGGGGKLKALKRKLRFLKAY-NH_2	261 ± 69	1.0
B72-1	AELAALEAELAALEGGGGGGGKL<u>A</u>ALKRKLRFLKAY-NH_2	130 ± 21	0.50
B72-2	AELAALEAELAALEGGGGGGGKLKALK<u>A</u>KLRFLKAY-NH_2	97 ± 38	0.37
B72-3	AELAALEAELAALEGGGGGGGKLKALKRKL<u>A</u>FLKAY-NH_2	67 ± 3	0.26
B72-4	AELAALEAELAALEGGGGGGGKLKALKRKLR<u>A</u>LKAY-NH_2	54 ± 15	0.21

[a] Alanine substitutions are underlined. [b] The peptide concentration is 5 μM. [c] Ratio to B72.

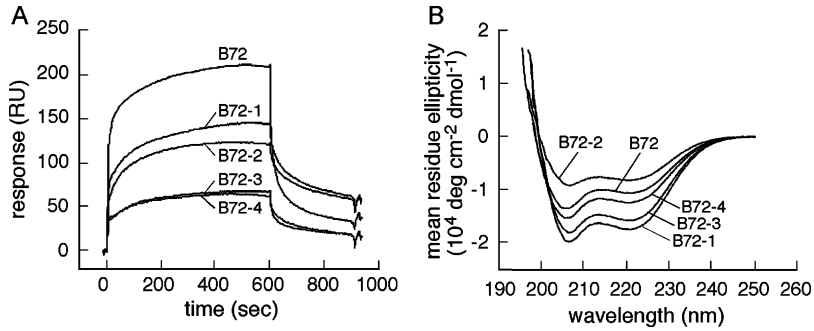

FIGURE 7: Effect of alanine substitutions on the binding of B72 to GM1 and helix formation. (A) SPR sensorgrams for the interaction of B72 and B72 mutants at 10 μM with GM1. (B) CD spectra of B72 and B72 mutants in TBS at pH 7.5. The peptide concentration was 100 μM.

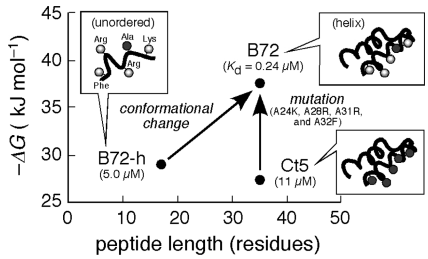

FIGURE 8: Changes in the Gibbs free energy between the complexes of B72, B72-h, and Ct5 with GM1. The ΔG value was calculated from the equation $\Delta G = -RT \ln K_d$, where $T = 298$ K.

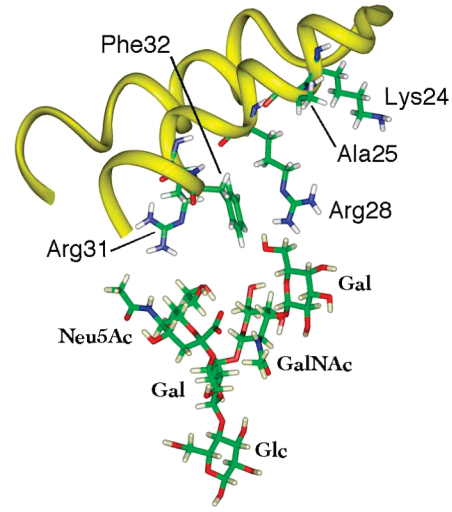

FIGURE 9: Deduced model for the interaction between B72 and pentasaccharide GM1. The side chains of Lys24, Ala25, Arg28, Arg31, and Phe32 in B72 are shown in a stick representation. The GM1 pentasaccharide structure was obtained from Protein Data Bank entry 3CHB.

B72 exhibited a decrease in the amount bound to asialo GM1 and GM2 (Figure 6), which means that a terminal Gal and Neu5Ac of GM1 are required for the interaction. CTB and p3 also bind to the terminal Gal and Neu5Ac of GM1 (*21, 22, 26*). X-ray structural data for the CTB−GM1 complex (Protein Data Bank entry 3CHB) show that the terminal Gal and Neu5Ac interacted with CTB. Therefore, these sugar residues are expected to interact with p3 or B72 in a similar manner. In fact, the binding of CTB to GM1 was competitively replaced with that of B72, and the concentration required for 50% inhibition was 1.1 μM (Supporting Information, Figure S3) (*26*). The molecular modeling shown in Figure 9 indicated that Lys24, Arg28, Arg31, and Phe32 in the C-terminal helix of B72 are arranged to interact with the terminal Gal and Neu5Ac in GM1. A guanidinium group of Arg can form a hydrogen bond with an OH group of the terminal Gal or Neu5Ac and/or salt bridge with a carboxyl group of Neu5Ac. The phenyl group of Phe can form a stack with the hydrophobic B face of the terminal Gal and/or acetoamido group of Neu5Ac.

In conclusion, oligosaccharide-binding peptides with a helix−loop−helix scaffold were selected and their specificities were investigated. One of the peptides exhibited an increase in binding affinity compared with a 15-mer peptide that we identified previously (*26*). The new peptide's helical structure contributed to its ability to recognize carbohydrates, and arginine and phenylalanine were found to be involved in its interaction with GM1. The GM1-binding amino acid residues in the α-helix enabled the peptide to fit GM1. Many antibodies and lectins achieve greater affinity for carbohydrates by displaying carbohydrate-binding residues with a structural scaffold (*33*). This is the first paper to demonstrate the advantages of the arrangement of carbohydrate-binding residues in the helix−loop−helix scaffold for increasing binding affinity.

ACKNOWLEDGMENT

We thank Prof. H. Yanagawa and Dr. N. Doi (Keio University) for providing the opportunity to use the CD spectrometer.

SUPPORTING INFORMATION AVAILABLE

A saturation binding curve of phages to GM1 determined via an ELISA (Figure S1), affinity of phages for various glycolipids (Table S1), amounts of B72 mutant peptides bound to GM1 (Figure S2), and competitive inhibition assay of peptides (Figure S3). This material is available free of charge via the Internet at http://pubs.acs.org.

REFERENCES

1. Varki, A. (1993) Biological roles of oligosaccharides: All of the theories are correct. *Glycobiology 3*, 97–130.
2. Kannagi, R., and Hakomori, S. (2001) A guide to monoclonal antibodies directed to glycotopes. *Adv. Exp. Med. Biol. 491*, 587–630.
3. Qiu, J. X., Kai, M., Padlan, E. A., and Marcus, D. M. (1999) Structure-function studies of an anti-asialo GM1 antibody obtained from a phage display library. *J. Neuroimmunol. 97*, 172–181.
4. Bradbury, A. R., and Marks, J. D. (2004) Antibodies from phage antibody libraries. *J. Immunol. Methods 290*, 29–49.
5. Dinh, Q., Weng, N. P., Kiso, M., Ishida, H., Hasegawa, A., and Marcus, D. M. (1996) High affinity antibodies against Le^x and sialyl Le^x from a phage display library. *J. Immunol. 157*, 732–738.
6. Mao, S., Gao, C., Lo, C. H., Wirsching, P., Wong, C. H., and Janda, K. D. (1999) Phage-display library selection of high-affinity human single-chain antibodies to tumor-associated carbohydrate antigens sialyl $Lewis^x$ and $Lewis^x$. *Proc. Natl. Acad. Sci. U.S.A. 96*, 6953–6958.
7. Wang, L., Radic, M. Z., Siegel, D., Chang, T., Bracy, J., and Galili, U. (1997) Cloning of anti-Gal Fabs from combinatorial phage display libraries: Structural analysis and comparison of Fab expression in pComb3H and pComb8 phage. *Mol. Immunol. 34*, 609–618.
8. Ravn, P., Danielczyk, A., Jensen, K. B., Kristensen, P., Christensen, P. A., Larsen, M., Karsten, U., and Goletz, S. (2004) Multivalent scFv display of phagemid repertoires for the selection of carbohydrate-specific antibodies and its application to the Thomsen-Friedenreich antigen. *J. Mol. Biol. 343*, 985–996.
9. Rojas, G., Talavera, A., Munoz, Y., Rengifo, E., Krengel, U., Angstrom, J., Gavilondo, J., and Moreno, E. (2004) Light-chain shuffling results in successful phage display selection of functional prokaryotic-expressed antibody fragments to N-glycolyl GM3 ganglioside. *J. Immunol. Methods 293*, 71–83.
10. Yamamoto, K., Maruyama, I. N., and Osawa, T. (2000) Cyborg lectins: Novel leguminous lectins with unique specificities. *J. Biochem. 127*, 137–142.
11. Yim, M., Ono, T., and Irimura, T. (2001) Mutated plant lectin library useful to identify different cells. *Proc. Natl. Acad. Sci. U.S.A. 98*, 2222–2225.
12. Yamada, S., Suzuki, Y., Suzuki, T., Le, M. Q., Nidom, C. A., Sakai-Tagawa, Y., Muramoto, Y., Ito, M., Kiso, M., Horimoto, T., Shinya, K., Sawada, T., Usui, T., Murata, T., Lin, Y., Hay, A., Haire, L. F., Stevens, D. J., Russell, R. J., Gamblin, S. J., Skehel, J. J., and Kawaoka, Y. (2006) Haemagglutinin mutations responsible for the binding of H5N1 influenza A viruses to human-type receptors. *Nature 444*, 378–382.
13. Stevens, J., Blixt, O., Tumpey, T. M., Taubenberger, J. K., Paulson, J. C., and Wilson, I. A. (2006) Structure and receptor specificity of the hemagglutinin from an H5N1 influenza virus. *Science 312*, 404–410.
14. DeGrado, W. F., Summa, C. M., Pavone, V., Nastri, F., and Lombardi, A. (1999) De novo design and structural characterization of proteins and metalloproteins. *Annu. Rev. Biochem. 68*, 779–819.
15. Baltzer, L., and Nilsson, J. (2001) Emerging principles of de novo catalyst design. *Curr. Opin. Biotechnol. 12*, 355–360.
16. Bolon, D. N., Voigt, C. A., and Mayo, S. L. (2002) De novo design of biocatalysts. *Curr. Opin. Chem. Biol. 6*, 125–129.
17. Gibas, C., and Subramaniam, S. (1997) Knowledge-based design of a soluble bacteriorhodopsin. *Protein Eng. 10*, 1175–1190.
18. Hosse, R. J., Rothe, A., and Power, B. E. (2006) A new generation of protein display scaffolds for molecular recognition. *Protein Sci. 15*, 14–27.
19. Uchiyama, F., Tanaka, Y., Minari, Y., and Tokui, N. (2005) Designing scaffolds of peptides for phage display libraries. *J. Biosci. Bioeng. 99*, 448–456.
20. Rosinski, J. A., and Atchley, W. R. (1999) Molecular evolution of helix-turn-helix proteins. *J. Mol. Evol. 49*, 301–309.
21. Merritt, E. A., Sarfaty, S., van den Akker, F., L'Hoir, C., Martial, J. A., and Hol, W. G. (1994) Crystal structure of cholera toxin B-pentamer bound to receptor GM1 pentasaccharide. *Protein Sci. 3*, 166–175.
22. Kuziemko, G. M., Stroh, M., and Stevens, R. C. (1996) Cholera toxin binding affinity and specificity for gangliosides determined by surface plasmon resonance. *Biochemistry 35*, 6375–6784.
23. Harder, T., Scheiffele, P., Verkade, P., and Simons, K. (1998) Lipid domain structure of the plasma membrane revealed by patching of membrane components. *J. Cell Biol. 141*, 929–942.
24. Yanagisawa, K. (2007) Role of gangliosides in Alzheimer's disease. *Biochim. Biophys. Acta 1768*, 1943–1951.
25. Matsubara, T., Ishikawa, D., Taki, T., Okahata, Y., and Sato, T. (1999) Selection of ganglioside GM1-binding peptides by using a phage library. *FEBS Lett. 456*, 253–256.
26. Matsubara, T., Iijima, K., Nakamura, M., Taki, T., Okahata, Y., and Sato, T. (2007) Specific Binding of GM1-Binding Peptides to High-Density GM1 in Lipid Membranes. *Langmuir 23*, 708–714.
27. Fujitani, N., Shimizu, H., Matsubara, T., Ohta, T., Komata, Y., Miura, N., Sato, T., and Nishimura, S. (2007) Structural transition of a 15 amino acid residue peptide induced by GM1. *Carbohydr. Res. 342*, 1895–1903.
28. Gram, H., Marconi, L. A., Barbas, C. F., III, Collet, T. A., Lerner, R. A., and Kang, A. S. (1992) In vitro selection and affinity maturation of antibodies from a naive combinatorial immunoglobulin library. *Proc. Natl. Acad. Sci. U.S.A. 89*, 3576–3580.
29. Greenfield, N., and Fasman, G. D. (1969) Computed circular dichroism spectra for the evaluation of protein conformation. *Biochemistry 8*, 4108–4116.
30. Suzuki, N., and Fujii, I. (1999) Optimization of the loop length for folding of a helix loop helix peptide. *Tetrahedron Lett. 40*, 6013–6017.
31. Fujii, I., Takaoka, Y., Suzuki, K., and Tanaka, T. (2001) A conformationally purified α-helical peptide library. *Tetrahedron Lett. 42*, 3323–3325.
32. Rockendorf, N., Bade, S., Hirst, T. R., Gorris, H. H., and Frey, A. (2007) Synthesis of a fluorescent ganglioside G(M1) derivative and screening of a synthetic peptide library for G(M1) binding sequence motifs. *Bioconjugate Chem. 18*, 573–578.
33. Weis, W. I., and Drickamer, K. (1996) Structural basis of lectin-carbohydrate recognition. *Annu. Rev. Biochem. 65*, 441–473.
34. Hyun, S., Kim, J., Kwon, M., and Yu, J. (2007) Selection and syntheses of tentacle type peptides as 'artificial' lectins against various cell-surface carbohydrates. *Bioorg. Med. Chem. 15*, 511–517.
35. Yang, J. T., Wu, C.-S. C., and Martinez, H. M. (1986) Calculation of protein conformation from circular dichroism. *Methods Enzymol. 130*, 208–269.
36. Vila, J. A., Ripoll, D. R., and Scheraga, H. A. (2000) Physical reasons for the unusual α helix stabilization afforded by charged or neutral polar residues in alanine-rich peptides. *Proc. Natl. Acad. Sci. U.S.A. 97*, 13075–13079.
37. Gronow, S., and Brade, H. (2001) Lipopolysaccharide biosynthesis: Which steps do bacteria need to survive? *J. Endotoxin Res. 7*, 3–23.
38. Rudiger, H., and Gabius, H. J. (2001) Plant lectins: Occurrence, biochemistry, functions and applications. *Glycoconjugate J. 18*, 589–613.
39. Love, K. R., and Seeberger, P. H. (2002) Carbohydrate arrays as tools for glycomics. *Angew. Chem., Int. Ed. 41*, 3583–3586.
40. Hirabayashi, J., and Kasai, K. (2002) Separation technologies for glycomics. *J. Chromatogr., B 771*, 67–87.
41. Feizi, T., Fazio, F., Chai, W., and Wong, C. H. (2003) Carbohydrate microarrays: A new set of technologies at the frontiers of glycomics. *Curr. Opin. Struct. Biol. 13*, 637–645.
42. Matsubara, T., and Sato, T. (2007) Identification of oligosaccharide-recognition molecules by phage-display technology. *Trends Glycosci. Glycotechnol. 19*, 121–132.
43. Lis, H., and Sharon, N. (1998) Lectins: Carbohydrate-specific proteins that mediate cellular recognition. *Chem. Rev. 98*, 637–674.

BI8000837